Fast second-order many-body perturbation method for extended systems

So Hirata*
Department of Chemistry and Department of Physics, Quantum Theory Project and The Center for Macromolecular Science and Engineering, University of Florida, Gainesville, Florida 32611, USA

Tomomi Shimazaki
Fracture and Reliability Research Institute, Graduate School of Engineering, Tohoku University, Sendai 980-8579, Japan
(Received 17 June 2009; revised manuscript received 24 July 2009; published 26 August 2009)

An application of second-order many-body perturbation theory to energies and energy bands of polymers is often hindered by the steep polynomial dependence of its computational cost on the number of wave vector sampling points (K) in the Brillouin zone (BZ). It is shown that a Hartree-Fock (HF) calculation with a large value of K (120 in the first BZ) followed by a second-order many-body perturbation calculation with a much smaller value ($K=6$) can lead to reliable, interpolated correlated energy bands and density of states of a polymer at less than 1% of the computational cost of the conventional approach. Quantitative simulations on photoelectron spectra of *trans*- and *cis*-polyacetylenes and polyethylene show that the correlated energy bands and densities of states thus obtained agree quantitatively with the observed and are significant (sometimes qualitative) improvements over the HF results. The energy bands and photoelectron spectra of polydiacetylene are predicted by this method to assist in the interpretation of future high-resolution measurements.

DOI: 10.1103/PhysRevB.80.085118 PACS number(s): 71.15.Dx, 71.20.−b, 31.15.xp

I. INTRODUCTION

In crystalline orbital (CO) theory,[1,2] an extended system of one-dimensional periodicity is viewed mathematically as a ring of K identical repeat units. A canonical CO in the Hartree-Fock (HF) theory,[3–7] therefore, resembles an eigenfunction of the quantum-mechanical particle-on-a-ring problem

$$\varphi_{pk}(\mathbf{r}) = K^{-1/2}\sum_{\mu}\sum_{m} C_{pk}^{\mu}\exp(ikma)\chi_{\mu}(\mathbf{r}-m\mathbf{a}), \qquad (1)$$

where $\mathbf{a}$ is the translational vector, $\chi_{\mu}(\mathbf{r}-m\mathbf{a})$ is the μth basis function centered in the mth unit cell, and C_{pk}^{μ} is an expansion coefficient to be determined variationally. Each orbital is associated with the wave vector (k) that is equal to the linear momentum of its electron and can take one of the following values:

$$k = \frac{2m}{K}, \quad \{m \in \mathbb{Z} | 0 \le m < K\}, \qquad (2)$$

where a unit of length is chosen such that $|\mathbf{a}|=\pi$. These k vectors characterize the elementary unit cell in the reciprocal space—the Brillouin zone (BZ)—and are evenly spaced. The number of wave vector sampling points (K) used in the BZ integrations can, therefore, be interpreted as the system size and should be commensurate with the distance reached by the effective interactions or the number of neighbors included in the lattice sums.

In an insulator, the direct Coulomb (J) interaction is the slowest-decaying component with distance (r) in the HF energy of an extended system, displaying an r^{-3} asymptote. It is usually necessary to take into account interactions up to at least the fifth nearest neighbors to achieve a converged lattice sum in a HF calculation for a nonpolar unit cell and much farther for a polar unit cell.[8] Accordingly, the number of k vectors (K) used in BZ integrations should be on the order of 10. Since the cost of performing BZ integrations are negligible in a HF calculation, these or even greater values of K can be used easily. Because the distinct k vectors are evenly spaced the trapezoidal rule works well for BZ integrations in one dimension, although other quadrature rules have also been applied.[9] In BZ integrations in two and three dimensions, the use of special points[10–12] is essential.

In contrast to the HF case, the cost of evaluating the electron-correlation energy of an extended system depends strongly on K.[13,14] For instance, the second-order many-body or Møller-Plesset perturbation theory—MBPT(2) or MP2—for an extended system[15–29] involves an $O(K^3)$ step, hampering its routine applications to extended systems. However, the dynamical correlation interactions exhibit a rapid r^{-6} decay[14,26] and it is reasonable to expect that far fewer nearest-neighbor cells need to be included in MP2 than in HF. It is, therefore, justifiable to use a large value of K only in the HF step followed by the MP2 step with a much smaller value of K. In our previous study, we proposed using only every nth k vectors of the HF step in the BZ integrations of the MP2 step.[30] Using this "mod-n" approximation with $K=20$ and $n=4$, we could reproduce the MP2 correlation energies of polyethylene and polyacetylene within 1% of the respective converged values at less than a tenth of the usual computational cost. MP2 correlation corrections to energy bands obtained were also computed accurately by this approximation.[30]

The purpose of this study is to demonstrate the practical utility of this mod-n approximation with large values of n and K in the first-principles simulations of photoelectron spectra of four polymeric materials: *trans*- and *cis*-polyacetylenes, polyethylene, and polydiacetylene. These spectra report energy bands and density of states, which are strongly influenced by electron correlation; the HF theory and density-functional theory (DFT) are often found to be inadequate. To obtain smooth and continuous energy bands and hence reliable density of states, one needs a large number of

k vectors, which, however, makes electron-correlation calculations unfeasible. Our mod-n approximation is a solution to this dilemma as one can obtain smooth energy bands at the HF level with a large value of K (such as 120 in this work) as well as correlation corrections to important bands at only every nth k vectors ($n=20$ in this work) at a dramatically reduced cost. Combining these HF and MP2 results, one can interpolate the MP2 quasiparticle energy bands that can subsequently be used to generate density of states, which explains the observed spectra quantitatively. It is estimated that the mod-20 approximation achieves a speedup by a factor of 100 or more.

II. COMPUTATIONAL METHOD

In the mod-n approximation,[30] the MP2 energy per unit cell (E^{MP2}) and quasiparticle energy ($e^{\mathrm{MP2}}_{pk_p}$) of the one-electron state (orbital) characterized by band p and wave vector k_p are given by

$$E^{\mathrm{MP2}} = E^{\mathrm{HF}} + K^{-1}n^3 \sum_{k_i\in K_n}\sum_{k_j\in K_n}\sum_{k_a\in K_n}\sum_{i,j,a,b} \frac{v^{ik_ijk_j}_{ak_abk_b} w^{ik_ijk_j*}_{ak_abk_b}}{e^{\mathrm{HF}}_{ik_i} + e^{\mathrm{HF}}_{jk_j} - e^{\mathrm{HF}}_{ak_a} - e^{\mathrm{HF}}_{bk_b}} \tag{3}$$

and

$$e^{\mathrm{MP2}}_{pk_p} = e^{\mathrm{HF}}_{pk_p} + n^2 \sum_{k_j\in K_n}\sum_{k_b\in K_n}\sum_{j,a,b} \frac{v^{pk_pjk_j}_{ak_abk_b} w^{pk_pjk_j*}_{ak_abk_b}}{e^{\mathrm{HF}}_{pk_p} + e^{\mathrm{HF}}_{jk_j} - e^{\mathrm{HF}}_{ak_a} - e^{\mathrm{HF}}_{bk_b}} + n^2 \sum_{k_j\in K_n}\sum_{k_b\in K_n}\sum_{i,j,b} \frac{v^{ik_ijk_j}_{pk_pbk_b} w^{ik_ijk_j*}_{pk_pbk_b}}{e^{\mathrm{HF}}_{pk_p} + e^{\mathrm{HF}}_{bk_b} - e^{\mathrm{HF}}_{ik_i} - e^{\mathrm{HF}}_{jk_j}}, \tag{4}$$

respectively. Here, E^{HF} and $e^{\mathrm{HF}}_{pk_p}$ denote the HF energy per unit cell and the HF energy of the one-electron state, i and j label occupied bands, a and b unoccupied (virtual) bands, and $v^{pk_pjk_j}_{ak_abk_b}$ and $w^{pk_pjk_j}_{ak_abk_b}$ are two-electron integrals over COs as defined in our previous paper.[14] These integrals vanish identically unless the following momentum conservation law is satisfied:

$$k_p + k_j - k_a - k_b = 2m, \quad \{m \in \mathbb{Z}\}. \tag{5}$$

The k summations (the BZ integrations) sample only every nth of all k vectors considered in the HF step. Hence, K_n denotes the following set of k vectors:

$$k = \frac{2nm}{K}, \quad \{m \in \mathbb{Z} | 0 \le nm < K\}, \tag{6}$$

where K is the number of k vectors used in the HF step. In this article, we stipulate that n evenly divides K so that the trapezoidal rule for the BZ integration continues to work well. The quasiparticle energies ($e^{\mathrm{MP2}}_{pk_p}$) are computed only at those k_p's that satisfy Eq. (6). Therefore, the mod-n approximation reduces the cost of evaluating both Eqs. (3) and (4) by a factor of n^3. Note, however, they are not the hotspot of the calculation (the integral transformation is) unless K is very large.

The mod-n MP2 calculations give quasiparticle energies on a sparse grid of k vectors, whereas the HF energy bands can be obtained on a fine grid with an arbitrarily large number of k vectors. To interpolate MP2 energy bands, we must first connect the HF energy points correctly to form smooth curves; simply connecting the ith lowest energy points for each i would result in curves that have nonphysical cusps at band crossings. However, this step can be carried out straightforwardly by inspection in a one-dimensional BZ insofar as K is sufficiently large and the correct connectivity is evident to human eyes (for two- and three-dimensional BZs, information about orbitals must be utilized). Once a smooth HF band ($e^{\mathrm{HF}}_{pk_p}$) is obtained on a fine grid of k vectors, the MP2 quasiparticle energy at k is interpolated by the following formula:

$$e^{\mathrm{MP2}}_{pk} = e^{\mathrm{HF}}_{pk} + (e^{\mathrm{MP2}}_{pk_1} - e^{\mathrm{HF}}_{pk_1})\frac{k-k_2}{k_1-k_2} + (e^{\mathrm{MP2}}_{pk_2} - e^{\mathrm{HF}}_{pk_2})\frac{k-k_1}{k_2-k_1}, \tag{7}$$

where k_1 and k_2 are the two nearest k vectors at which MP2 quasiparticles energies are explicitly evaluated in the mod-n approximation. Because an MP2 correction is made to a state, pairing $e^{\mathrm{MP2}}_{pk_2}$ and $e^{\mathrm{HF}}_{pk_2}$ or $e^{\mathrm{MP2}}_{pk_1}$ and $e^{\mathrm{HF}}_{pk_1}$ can be done without any difficulty.

III. RESULTS AND DISCUSSION

The HF/6-31G* calculations with $K=120$ were performed for the energy bands of *trans*- and *cis*-polyacetylenes (C_2H_2 unit cell), polyethylene (C_2H_4), and polydiacetylene (C_4H_2) at their respective equilibrium geometries obtained by the Becke3-Lee-Yang-Parr (B3LYP) DFT method with the 6-31G* basis set.[31–33] The short- and long-range interactions were summed in the sixth ($S=6$) and twentieth ($L=20$) nearest-neighbor approximations[14] in *trans*-polyacetylene. For *cis*-polyacetylene and polydiacetylene, the corresponding parameters were $S=3$ and $L=7$. For polyethylene, $S=6$ and $L=10$ were used. Subsequently, MP2/6-31G* energy-band calculations in the frozen-core approximation were carried out in the mod-20 scheme, providing quasiparticle energies on a sparse grid of k vectors: $k=0$, 1/3, 2/3, 1, 4/3, and 5/3. The densities of states were computed as histograms with the bin size of 10^{-4} a.u., using the HF and interpolated MP2 energy bands. They were convoluted with a Gaussian function with a full width at half maximum of 1.6 eV for polyacetylenes and polyethylene and 1.2 eV for polydiacetylene.

A. *Trans*-polyacetylene

Figure 1 plots the CPU time spent in the mod-n MP2/6-31G* calculation of *trans*-polyacetylene as a function of n. A large and monotonic reduction in the computational cost is observed with increasing n. The mod-20 approximation with $K=120$ is estimated to result in at least a 100-fold reduction in the CPU time, making MP2 quasiparticle energy calculations of polymers with small unit cells routinely feasible. The slope of the plots is between −2.4 and

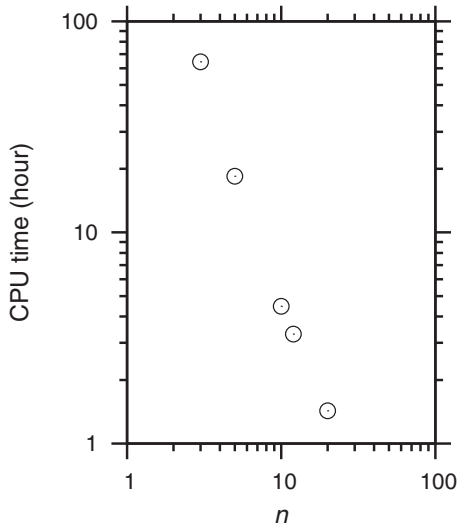

FIG. 1. The CPU time spent by the mod-n MP2/6-31G* calculation of *trans*-polyacetylene as a function of n on a 3.2-GHz Intel Xeon EM64T processor with a 4-GB RAM.

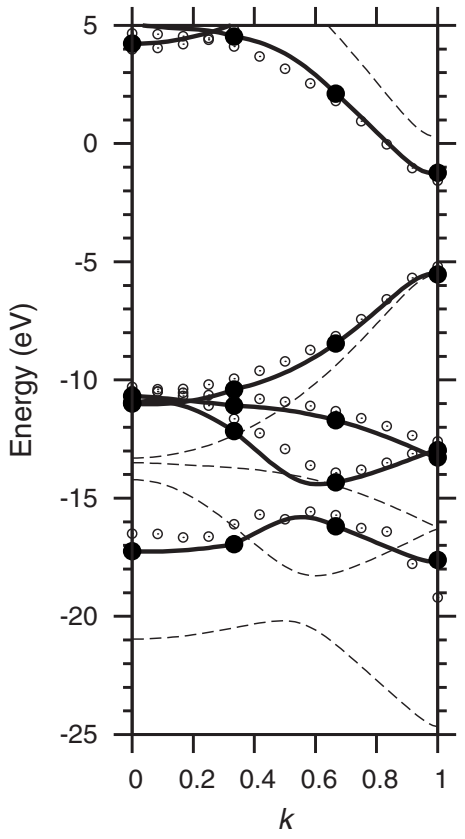

FIG. 2. The HF/6-31G* (broken curves) and MP2/6-31G* (solid curves) energy bands of *trans*-polyacetylene. The highest-lying band shown is the conduction band. The HF calculation was carried out with $K=120$. The MP2 calculation was performed in the mod-20 approximation, giving quasiparticle energies (filled circles) at $k=0$, 1/3, 2/3, 1, 4/3, and 5/3. The MP2 bands were interpolated according to the procedure described in the text. The MP2/6-31G* quasiparticle energies obtained in the mod-5 approximation (open circles) are also superimposed.

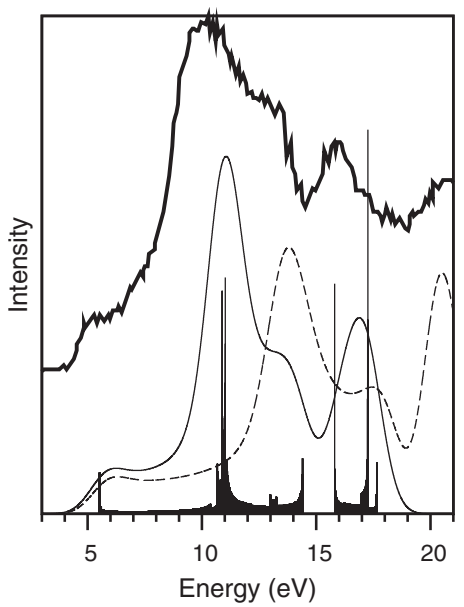

FIG. 3. The observed (Ref. 34) (thick solid curve; elevated for clarity), the HF/6-31G* calculated (thin broken curve), and the MP2/6-31G* calculated (thin solid curve) photoelectron spectra of *trans*-polyacetylene. The MP2/6-31G* density of states is also superimposed.

−1.6. The former value has been obtained with the $n=3$ and 5 and the latter with $n=12$ and 20. Equations (3) and (4) suggest the theoretical speedup of n^3. The actual speedup ($n^{2.4}$) obtained approaches this theoretical limit in the case of a small n and a large K, where Eqs. (3) and (4) are the rate determining step.

Figure 2 compares the energy bands of *trans*-polyacetylene obtained by various methods. The interpolated MP2 occupied energy bands lie higher and unoccupied bands lower than the corresponding HF energy bands by as much as a few eV.[17] In addition, the correlation corrections are dependent on k vectors, considerably contracting band widths. A comparison between the mod-5 and mod-20 MP2 energy bands shows that the simple interpolation scheme of Eq. (7) works well. For instance, the MP2 corrections to the lowest-lying band in Fig. 2 are greater toward the right edge of the figure ($k=1$). The interpolation of the four MP2 quasiparticle energies using the continuous HF bands suggests a maximum at $k\approx 0.6$, which is supported by the mod-5 result. Note, however, that the latter suffers from some noise caused by the fact that Eq. (4) is increasingly ill conditioned away from the Fermi level.[22] While the interpolation of the mod-20 MP2 energy band does not agree perfectly with the mod-5 MP2 energy band, the deviation is on the same order of magnitude as the noise in the latter. In the context of obtaining density of states, the mod-5 MP2 results (roughly equivalent to a $K=24$ MP2 calculation) do not have a sufficient resolution to discern bands near $k=0$. Our scheme enables us to correctly classify energy points to bands by virtue of having a large value of K at the HF step and at the same time to avoid an explosive increase in the computational cost of the MP2 step.

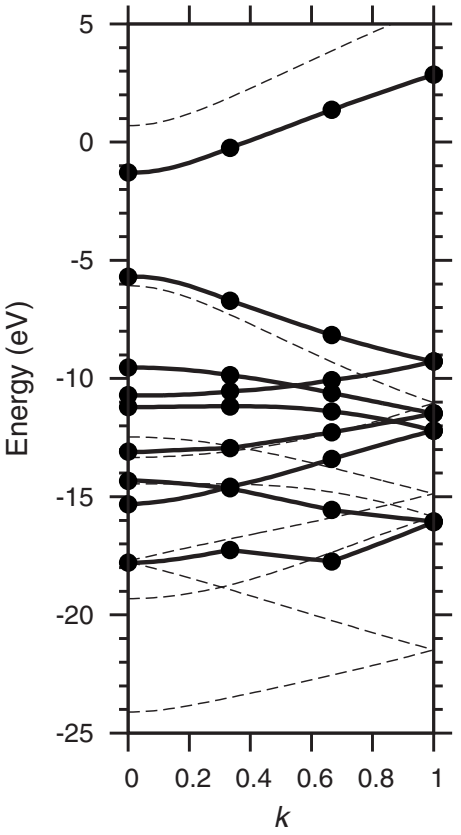

FIG. 4. The HF/6-31G* (broken curves) and MP2/6-31G* (filled circles and solid curves) energy bands of *cis*-polyacetylene. The highest-lying band shown is the conduction band. See also the caption of Fig. 2.

Figure 3 compares HF and MP2 densities of states with an observed photoelectron spectrum.[34] With the exception of the onset at 5.5 eV, the peak positions in the HF density of states are overestimated by a few eV. The MP2 density of states is in excellent agreement with the observed both in peak positions and intensities. In our previous B3LYP study,[31] the good agreement was obtained both in peak positions and intensity profile. The agreement in peak positions is to a great extent due to the cancellation of errors in ionization energies between semilocal DFT and HF. In contrast, the agreement between MP2 and the experiment must be much less due to such effects.

The peak at 5.5 eV can be assigned to the weak van Hove singularity in the density of states caused by the plateau of energy-band 1 at $k=1$ (the occupied energy bands are numbered in the decreasing order of their maximum energies). The most intense, broad peak at about 10 eV is due to three van Hove singularities caused by energy-bands 1, 2, and 3 at $k=0$. The shoulder at 13 eV is assignable to the singularity caused by the minimum of energy-band 3 at $k=0.6$. The dips in the measured spectrum at about 15 and 18 eV are assignable to band gaps between energy-bands 3 and 4 and between 4 and 5, respectively. The energy-band 4 gives rise to three van Hove singularities in the density of states and they contribute to the single observed peak at 16 eV.

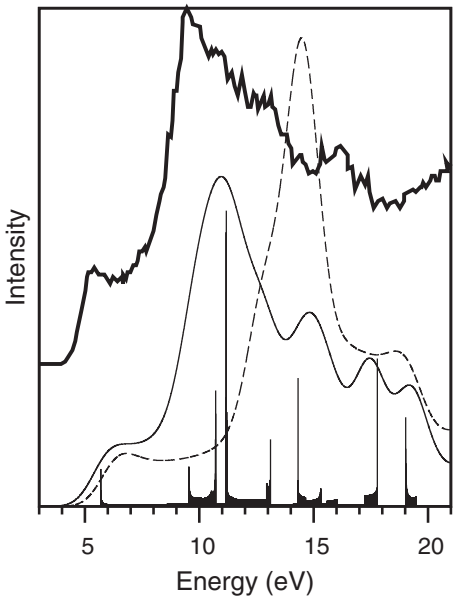

FIG. 5. The observed (Ref. 34) (thick solid curve; elevated for clarity), the HF/6-31G* calculated (thin broken curve), and the MP2/6-31G* calculated (thin solid curve) photoelectron spectra of *cis*-polyacetylene. The MP2/6-31G* density of states is also superimposed.

B. *Cis*-polyacetylene

As in the case of the *trans* isomer, the MP2 occupied energy bands of *cis* isomer are invariably shifted upward from the HF ones and their widths are contracted (Fig. 4). The conduction band is lowered and the fundamental band gap is thus significantly reduced upon inclusion of electron correlation. As the occupied band energies become lower, the MP2 and HF band shapes deviate from each other considerably and the interpolation tends to yield nonphysical rugged curves. To improve on these deeper bands, the use of an alternative interpolation scheme may not be sufficient and a more accurate, well-conditioned correlation correction is probably necessary.

The HF and MP2 densities of states (Fig. 5) differ from each other not only in peak positions but also in intensity profile. The HF density of state has little resemblance with the observed photoelectron spectrum,[34] whereas the MP2 density of state is in good agreement with the observed. MP2 is capable of reproducing slight differences in the overall appearance of the spectra between the *trans* and *cis* isomers. Specifically, the spectrum of the *cis* isomer is less structured and characterized by shallower dips at about 13 and 18 eV. These features are ascribed to the more congested density of states in the *cis* isomer. The 5.5- and 9.5-eV peaks are primarily assigned to the van Hove singularities associated with energy-bands 1 ($k=0$) and 4 ($k=0.3$), respectively. The dip at about 18 eV is caused by the energy gap between bands 8 and 9 (not shown). Again, the agreement in peak positions between B3LYP and experiment seen in our previous work[31] is largely fortuitous, although the agreement in intensity profile may be less so.

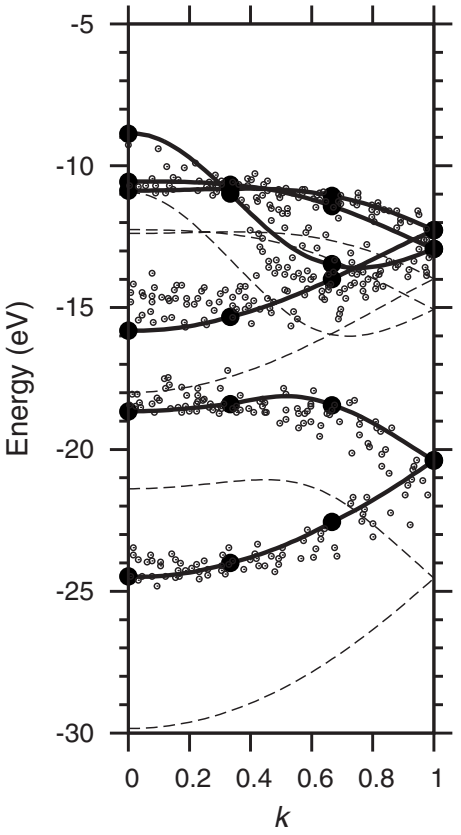

FIG. 6. The HF/6-31G* (broken curves) and MP2/6-31G* (filled circles and solid curves) energy bands of polyethylene. The highest-lying band is the valence band. See also the caption of Fig. 2. The positions of the observed angle-resolved photoelectron peaks (Ref. 39) of long *n* alkanes (open circles) are also plotted.

C. Polyethylene

The photoelectron spectra of polyethylene were interpreted in detail by Sun and Bartlett[35] on the basis of their periodic MP2 calculation (see also Delhalle *et al.*,[36] Springborg and Lev,[37] and Miao *et al.*[38]). It was necessary for them to use a large value of K (41) and, consequently, only a small basis set (6-31G) could be employed in their density-of-states calculations. In our mod-20 calculations, an MP2/6-31G* calculation was easily completed in less than 2 h of CPU time.

As seen in Fig. 6, the MP2 occupied energy bands are higher lying and more contracted than the HF ones. The MP2 conduction band (not shown) lies lower than the HF counterpart by ≈ 1 eV. Unlike in polyacetylenes, the correlation corrections in polyethylene are relatively uniform. Hence, the sparse MP2 energy points can be interpolated accurately and the quantitative agreement can be obtained between the interpolated MP2 energy bands and angle-resolved photoelectron spectra of long *n* alkanes.[39] The observed peak positions have been shifted upwards by 2 eV in Fig. 6, but this is justified by a more recent measurement[40] on n-$C_{44}H_{90}$ that agrees excellently with the present MP2 calculation without a shift. Note that the two lowest-lying bands span 9 eV (from 21 to 30 eV) according to HF, whereas the corresponding MP2 bands span only 6 eV (from 18 to 24 eV). The latter is supported by both experiments.[39,40]

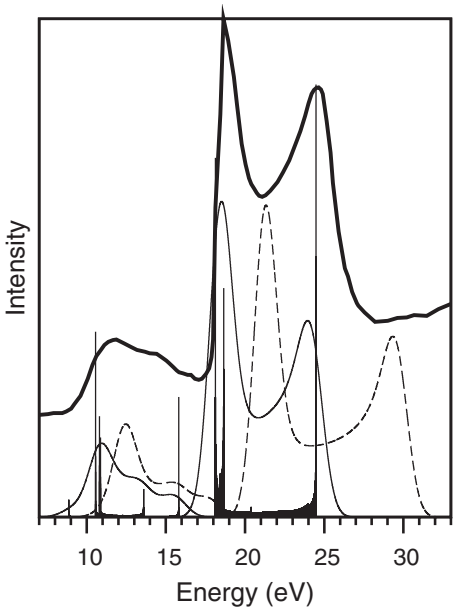

FIG. 7. The observed photoelectron spectrum (Ref. 41) of n-$C_{44}H_{90}$ (thick solid curve; elevated for clarity) and the HF/6-31G* (thin broken curve) and MP2/6-31G* calculated (thin solid curve) photoelectron spectra of polyethylene. The MP2/6-31G* density of states is also superimposed. The calculated density of states due to the four highest-lying occupied bands is multiplied by a factor of 0.1.

Figure 7 compares an observed photoelectron spectrum[41] of n-$C_{36}H_{74}$ (the work function is estimated to be 4.5 eV according to Ref. 36) with the spectra of polyethylene simulated by HF and MP2. While the HF theory can reproduce the overall intensity profile qualitatively correctly, the quantitative agreement requires a correlated theory. For instance, the separation between the two most intense peaks is 5.6 eV according to the experiment,[41] whereas it is evaluated to be 7.9 eV by HF and 5.4 eV by MP2. See Sun and Bartlett[35] for complete band assignments.

D. Polydiacetylene

Figure 8 shows the energy bands of polydiacetylene computed by HF and MP2. Not surprisingly, they have more similarities with those of polyacetylenes than those of polyethylene. While the MP2 correction to the highest occupied state at $k=0$ is small, it is greater elsewhere, making the MP2 bands contracted by a factor of about 1/3 as compared with the HF bands. The conduction band is more strongly affected by electron correlation than the valence band.

The HF and MP2 densities of states are compared with an observed photoelectron spectrum[42] of polydiacetylene in Fig. 9. All experimental spectra[42–46] including the one in Fig. 9 are measured for polymers with large organic ligands, giving rise to additional peaks in the valence region. This together with the low resolution of the spectra makes their interpretation "hopeless"[47] without assistance from a quantitative prediction. The HF and MP2 densities of states do not look alike and there is no apparent superiority of the MP2 spectrum to the HF one in comparison with the experiment. In light of

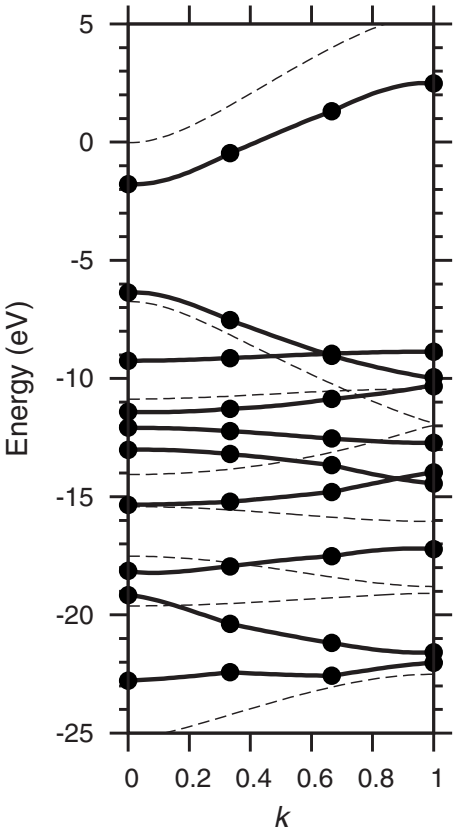

FIG. 8. The HF/6-31G* (broken curves) and MP2/6-31G* (filled circles and solid curves) energy bands of polydiacetylene. The highest-lying band is the conduction band. See also the caption of Fig. 2.

the results of polyacetylenes and polyethylene, however, we should base our assignments on the MP2 density of state.

The conspicuous dip in the intensity at about 20 eV is assignable to the band gap between energy-bands 7 and 8. The intense peak at about 10 eV is due to the rather flat energy-band 2. Its shoulder at about 6 eV is assigned to the van Hove singularity caused by energy-band 1 at $k=0$. In between (11–20 eV), there are five energy-bands (bands 3–7) with at least four distinct peaks in the computed spectrum, which explains rugged intensity profile in the observed spectrum. Our spectrum predicted by MP2 will be helpful in interpreting high-resolution spectra of unsubstituted polydiacetylene when they are measured in the future.

IV. CONCLUSION

Since electron correlation decays with distance much more rapidly than direct Coulomb interactions, the number

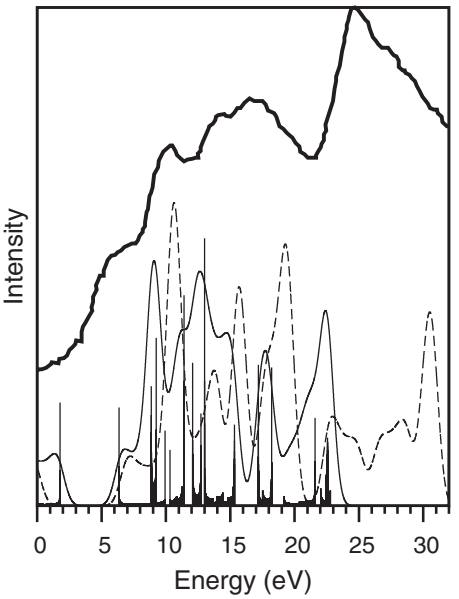

FIG. 9. The observed photoelectron spectrum (Ref. 42) of substituted polydiacetylene (thick solid curve; elevated for clarity) and the HF/6-31G* (thin broken curve) and MP2/6-31G* calculated (thin solid curve) photoelectron spectra of polydiacetylene. The MP2/6-31G* density of states is also superimposed.

of neighbors that need to be included in the lattice sums can be much smaller in MP2 than in HF. This suggests that the number of wave vector sampling points (K) in the BZ integrations—the measure of system size—in MP2 can be reduced by a large factor from a typical value necessary in the HF step. The MP2 quasiparticle energies on a sparse grid of wave vectors can be interpolated with the aid of the HF energies on a fine grid. When K needs to be large, a reduction of K in the MP2 step by a factor of as great as 20 is allowable with a 100-fold or greater speedup, making MP2 calculations for polymers routinely feasible. With this fast MP2, we have performed quantitative simulations and made peak assignments of photoelectron spectra of *trans*- and *cis*-polyacetylenes, polyethylene, and polydiacetylene. MP2 invariably reduces the errors in the peak positions from 5 eV or more in HF to 1–2 eV and improves the intensity profiles sometimes dramatically.

ACKNOWLEDGMENTS

This work was supported by the National Science Foundation (Grant No. CHE-0844448), the Department of Energy (Grant No. DE-FG02-04ER15621), and the American Chemical Society Petroleum Research Fund (Grant No. 48440-AC6). S.H. is a Camille Dreyfus Teacher-Scholar.

*hirata@qtp.ufl.edu

[1] J. Q. Sun and R. J. Bartlett, Top. Curr. Chem. **203**, 129 (1999).
[2] B. Champagne, in *Molecular Simulation Methods for Predicting Polymer Properties*, edited by V. Galiatsatos (Wiley, New York, 2005), pp. 1–46.
[3] G. Del Re, J. Ladik, and G. Biczó, Phys. Rev. **155**, 997 (1967).
[4] J.-M. André, L. Gouverneur, and G. Leroy, Int. J. Quantum Chem. **1**, 427 (1967).
[5] J.-M. André, L. Gouverneur, and G. Leroy, Int. J. Quantum Chem. **1**, 451 (1967).
[6] J. M. André, J. Chem. Phys. **50**, 1536 (1969).
[7] J. J. Ladik, *Quantum Theory of Polymers as Solids* (Plenum, New York, 1988).
[8] J. Delhalle, L. Piela, J. L. Brédas, and J.-M. André, Phys. Rev. B **22**, 6254 (1980).
[9] D. Jacquemin, B. Champagne, J. M. André, E. Deumens, and Y. Öhrn, J. Comput. Chem. **23**, 1430 (2002).
[10] D. J. Chadi and M. L. Cohen, Phys. Rev. B **8**, 5747 (1973).
[11] H. J. Monkhorst and J. D. Pack, Phys. Rev. B **13**, 5188 (1976).
[12] F. E. Harris, J. Phys.: Condens. Matter **14**, 621 (2002).
[13] S. Hirata, I. Grabowski, M. Tobita, and R. J. Bartlett, Chem. Phys. Lett. **345**, 475 (2001).
[14] S. Hirata, R. Podeszwa, M. Tobita, and R. J. Bartlett, J. Chem. Phys. **120**, 2581 (2004).
[15] A. B. Kunz, Phys. Rev. B **6**, 606 (1972).
[16] S. Suhai, Chem. Phys. Lett. **96**, 619 (1983).
[17] S. Suhai, Phys. Rev. B **27**, 3506 (1983).
[18] S. Suhai, Phys. Rev. B **52**, 1674 (1995).
[19] C.-M. Liegener, J. Phys. C **18**, 6011 (1985).
[20] C.-M. Liegener, J. Chem. Phys. **88**, 6999 (1988).
[21] Y.-J. Ye, W. Förner, and J. Ladik, Chem. Phys. **178**, 1 (1993).
[22] J. Q. Sun and R. J. Bartlett, J. Chem. Phys. **104**, 8553 (1996).
[23] J.-Q. Sun and R. J. Bartlett, J. Chem. Phys. **107**, 5058 (1997).
[24] J. Q. Sun and R. J. Bartlett, J. Chem. Phys. **106**, 5554 (1997).
[25] S. Hirata and S. Iwata, J. Chem. Phys. **109**, 4147 (1998).
[26] P. Y. Ayala, K. N. Kudin, and G. E. Scuseria, J. Chem. Phys. **115**, 9698 (2001).
[27] R. Pino and G. E. Scuseria, J. Chem. Phys. **121**, 2553 (2004).
[28] R. Pino and G. E. Scuseria, J. Chem. Phys. **121**, 8113 (2004).
[29] A. F. Izmaylov and G. E. Scuseria, Phys. Chem. Chem. Phys. **10**, 3421 (2008).
[30] T. Shimazaki and S. Hirata, Int. J. Quantum Chem. **109**, 2953 (2009).
[31] S. Hirata, H. Torii, and M. Tasumi, Phys. Rev. B **57**, 11994 (1998).
[32] S. Hirata and S. Iwata, J. Chem. Phys. **108**, 7901 (1998).
[33] M. Tobita, S. Hirata, and R. J. Bartlett, J. Chem. Phys. **114**, 9130 (2001).
[34] K. Kamiya, T. Miyamae, M. Oku, K. Seki, H. Inokuchi, C. Tanaka, and J. Tanaka, J. Phys. Chem. **100**, 16213 (1996).
[35] J. Q. Sun and R. J. Bartlett, Phys. Rev. Lett. **77**, 3669 (1996).
[36] J. Delhalle, J. M. Andre, S. Delhalle, J. J. Pireaux, R. Caudano, and J. J. Verbist, J. Chem. Phys. **60**, 595 (1974).
[37] M. Springborg and M. Lev, Phys. Rev. B **40**, 3333 (1989).
[38] M. S. Miao, P. E. Van Camp, V. E. Van Doren, J. J. Ladik, and J. W. Mintmire, Phys. Rev. B **54**, 10430 (1996).
[39] N. Ueno, K. Seki, N. Sato, H. Fujimoto, T. Kuramochi, K. Sugita, and H. Inokuchi, Phys. Rev. B **41**, 1176 (1990).
[40] D. Yoshimura, H. Ishii, Y. Ouchi, E. Ito, T. Miyamae, S. Hasegawa, K. K. Okudaira, N. Ueno, and K. Seki, Phys. Rev. B **60**, 9046 (1999).
[41] J. J. Pireaux, S. Svensson, E. Basilier, P.-Å. Malmqvist, U. Gelius, R. Caudano, and K. Siegbahn, Phys. Rev. A **14**, 2133 (1976).
[42] J. Knecht, B. Reimer, and H. Bässler, Chem. Phys. Lett. **49**, 327 (1977).
[43] D. Bloor, G. C. Stevens, P. J. Page, and P. M. Williams, Chem. Phys. Lett. **33**, 61 (1975).
[44] J. Knecht and H. Bässler, Chem. Phys. **33**, 179 (1978).
[45] G. C. Stevens, D. Bloor, and P. M. Williams, Chem. Phys. **28**, 399 (1978).
[46] A. A. Murashov, E. A. Silinsh, and H. Bässler, Chem. Phys. Lett. **93**, 148 (1982).
[47] A. Karpfen, J. Phys. C **13**, 5673 (1980).